

## MODELLING HYDROGEN DIFFUSION NEAR CRACK TIP IN METALS: IMPLICATIONS IN SLOW STRAIN RATE TESTING

J.Toribio\* and V. Kharin\*

Stress-assisted hydrogen diffusion near crack tip is analysed with reference to hydrogen assisted cracking (HAC) of metals. The study is focused on diffusion under dynamic loading with special emphasis on slow strain rate testing conditions. A numerical procedure is used to simulate crack-tip hydrogen concentration distributions affected by near-tip elastoplastic stress fields. Taking the sustained load hydrogen distribution as the reference one, the effects of loading dynamics on hydrogen accumulation in the fracture process zone are elucidated. Results are discussed with relation to accelerated HAC testing under transient loading. Conclusions are drawn regarding limitations on accelerated testing procedures to provide reasonable conservatism of evaluation of materials resistance against HAC.

### INTRODUCTION

Hydrogen is known to be a strong promoter of metals fracture (1). One of the key items of the studies of hydrogen assisted cracking (HAC) concerns about the transport mode which controls hydrogen accumulation in crack tip fracture process zone (FPZ). Stress-assisted hydrogen diffusion in metal can be responsible for the kinetics of HAC (2,3). Modelling of hydrogen accumulation in the FPZ has received considerable attention, but mainly with respect to sustained load (2,4).

The role of transient stress fields in diffusion is of interest, in particular, for justification of accelerated testing of materials susceptibility to HAC using rising load slow strain rate testing (SSRT), cf. (5), in contrast to sustained loading. There are two factors which compete to fulfil a rupture criterion: the kinetics of diffusion and the dynamics of stress-strain evolution. In general, faster loading leaves less time for hydrogen to reach the FPZ and fracture occurs more for mechanical reasons with lower effect of hydrogen than under slower rising load conditions. This can cause underestimation of deleterious action of hydrogen. However, at rather slow loading the delay of FPZ hydrogenation may be negligible so that the hydrogenous harm could develop completely. Modelling of near tip diffusion under SSRT should be helpful to gain insight about the role of interaction of diffusion kinetics and load dynamics in HAC.

---

\* Department of Materials Science, University of La Coruña, E.T.S.I. Caminos, Campus de Elviña, 15192 La Coruña, Spain.

BASIC MODEL CONSIDERATIONSDiffusional Theory of HAC

Hydrogen-assisted local rupture occurs when in a relevant material's cell the concentration reaches a critical value controlled, in general (3,5), by the principal stresses and strains  $\sigma_i$  and  $\varepsilon_i$  ( $i = 1,2,3$ ),  $C_{cr} = C_{cr}(\sigma_i, \varepsilon_i)$ . Fracture mechanics is based on the fact (6,7) that elastoplastic stress-strain field near crack tip, at least as close as few values of crack tip opening displacement (CTOD)  $\delta_t$ , is self-similar and thus can be represented by material-dependent functions of spatial coordinates  $(x,y)$  and CTOD:

$$\sigma_i = \sigma_i^*(x/\delta_t, y/\delta_t), \quad \varepsilon_i = \varepsilon_i^*(x/\delta_t, y/\delta_t) \quad (1)$$

Under small scale yielding and monotonous load inelastic near-tip state is controlled by the leading term of the outer elastic field defined by stress intensity factor (SIF)  $K$  which can replace CTOD in Eqs. (1) according to the relation (7,8):

$$\delta_t = 0.6 \frac{K^2}{E\sigma_Y} \quad (2)$$

where  $E$  is the Young modulus and  $\sigma_Y$  the yield strength. SIF represents the role of applied loads in crack tip and may vary with time  $t$ . Summarising, the opening mode crack situated along the  $x$ -axis is supposed to grow provided hydrogen concentration in some responsible location at  $x = x_c$  attains the critical level:

$$C(x_c, t) = C_{cr}(K(t), x_c) \quad (3)$$

where a suitable value of  $x_c$  must be available (2,4,9).

Hydrogenation is described by stress-assisted diffusion equation (2-4,9):

$$\frac{\partial C(x,t)}{\partial t} = D \left( \frac{\partial^2 C(x,t)}{\partial x^2} - \Omega \frac{\partial \sigma(x,t)}{\partial x} \frac{\partial C(x,t)}{\partial x} \right) \quad \left( \Omega = \frac{V_H}{RT} \right) \quad (4)$$

where  $D$  is diffusion coefficient and  $V_H$  the partial molal volume of hydrogen in metal,  $R$  the universal gas constant,  $T$  the absolute temperature, and  $\sigma$  the hydrostatic stress,  $\sigma = \sigma(K(t), x)$ . Hydrogen activity in the near tip environment is supposed capable to maintain on the metal surface equilibrium concentration  $C_\Gamma$  (3). Then, with crack tip fixed at  $x = 0$  the boundary condition for diffusion is:

$$C(x = 0, t) = C_\Gamma \quad \text{with} \quad C_\Gamma = C_0 \exp(\Omega \sigma_0(t)) \quad (5)$$

where  $C_0$  is equilibrium concentration in stress-free metal (2-4,9) and  $\sigma_0 = \sigma(x=0)$ .

Local rupture repeatedly occurs whilst concentration  $C(x,t)$  from Eq. (4) can satisfy the criterion Eq. (3) after diffusion times  $\Delta t$ . Then a crack advances by

increments  $\Delta l$  which render macroscopic crack growth rate  $v = \Delta l / \Delta t$ . Impossibility to solve Eq. (3) for finite time means crack arrest ( $v = 0$ ).

Sustained Load Case

At  $K = const$  Laplace transform provides the short- and long-time asymptotic solutions of the problem Eqs. (4) and (5),  $C_{as}$  and  $C_{al}$  correspondingly (cf. (9)):

$$\left\{ \begin{matrix} C_{as} \\ C_{al} \end{matrix} \right\} = C_T \left\{ \begin{matrix} \exp\left(\frac{\Omega}{2} (\sigma(K,x) - \sigma_0(K))\right) \\ \exp(\Omega (\sigma(K,x) - \sigma_0(K))) \end{matrix} \right\} \operatorname{erfc}\left(\frac{x}{2\sqrt{Dt}}\right) \quad (6)$$

The accurate solution of the diffusion problem gradually traverses with time from one asymptote to another. The second of them exactly gives the known (2-4) equilibrium hydrogen distribution  $C_\infty(K,x)$  as the steady-state solution of Eq. (4) achieved when  $t \rightarrow \infty$ . It defines the extreme hydrogenation at given SIF. Then, using  $C_\infty(K,x)$  in Eq. (3), it yields the equation to find the upper limit of  $K$  with which crack growth rate  $v = 0$  since this means satisfaction of the rupture criterion at  $\Delta t = \infty$ . Thus,  $C_\infty$  determines the threshold SIF value  $K_{th}$  for HAC.

Common test technique to determine  $K_{th}$  by trying a series of sustained SIF values  $K_Q^{(i)}$  ( $i = 1, \dots, n$ ) if crack does start to grow within certain time  $t_B$  looks like the route to solve experimentally Eq. (3) for steady-state left hand part. Roughly speaking, this requires total testing time  $t_T \sim n t_B$ . Diffusion concept of HAC suggests that to render valid  $K_{th}$  the value  $t_B$  must be about the diffusion time  $t_{ss}$  to attain the steady-state concentration in the point of interest with reasonable accuracy:  $C(x_c, t_{ss}) \approx C_\infty(x_c)$ . If, for definiteness, we fix the latter as attainment of 95% of steady-state level, then long-time asymptote Eq. (6) renders the estimate  $D t_{ss} / x_c^2 > 130$ . Note, this is a well lower bound because  $C_{al}(t)$  evaluates hydrogenation rate in excess.

SSRT with Constant Loading Rate

It is tempting to reduce  $K_{th}$ -testing expenses omitting a series of  $n$  tests with constant  $K_Q^{(i)}$  by conducting a single one with rising load, e.g., at constant SIF rate  $K^\bullet$ , to pass the whole SIF range up to detecting crack growth at SIF  $K_R$  which could be the HAC threshold. To be the adequate threshold, it would be necessary that concentration at  $t_R = K_R / K^\bullet$  reached the steady-state level  $C_\infty(K_R, x_c)$  with about the same accuracy as in sustained load test. Apparently, to obtain valid  $K_{th}$  it must be  $t_R > t_{ss}$  which possesses a limitation on admissible SIF rates in SSRT  $K^\bullet < K_R / t_{ss}$ . Further modelling should provide more insight into the matter.

In SSRT with  $K(t) = K^\bullet t$  diffusion proceeds near a tip of a crack produced by fatigue at maximum cyclic SIF  $K_{max}$ . Cyclic stability of near tip fields (10) reasons to start with the stress state given at  $t = 0$  by large-strain elastoplastic solution for a crack unloaded from  $K_{max}$  to zero (7), whereas at  $K \geq K_{max}$

monotonous load one (6) is used (Fig. 1, bold lines). These solutions display steep stress gradient at  $0 < x < x_m$  and a mild one at  $x_m \leq x \leq x_f$ , where  $x_m = \alpha \delta_t$  is the point of maximum absolute value of hydrostatic stress  $\sigma_m(t)$ , and  $x_f = 10\delta_t$  taken as the remote border of the zone of interest. At  $K < K_{max}$  CTOD is (8)

$$\delta_t = \delta_{max} \left[ 1 - \frac{1}{2} \left( 1 - \frac{K}{K_{max}} \right)^2 \right] \quad (7)$$

For  $K \geq K_{max}$  Eq. (2) is valid. Accounting for crack blunting the factor  $\alpha$  varies from 0.85 at  $K = 0$  to 1.5 at  $K \geq K_{max}$ , whereas  $\sigma_m(K=0) = -1.7 \sigma_Y$  and  $\sigma_m(K \geq K_{max}) = 2.5 \sigma_Y$  (6,7). At  $0 < K < K_{max}$  stress field parameters  $\sigma_m$  and  $x_m$  may be obtained by interpolation (Fig. 1). The suitable form of Eq. (4) is:

$$\frac{\partial C}{\partial \tau} = \left[ \frac{x_R}{x_m(t)} \right]^2 \left\{ \frac{\partial^2 C}{\partial \xi^2} - \left( \Omega \frac{\partial \sigma}{\partial \xi} - \frac{x_m \dot{x}_m}{D} \xi \right) \frac{\partial C}{\partial \xi} \right\} \quad (8)$$

where  $\tau = Dt/x_R^2$ ,  $x_R = x_m(K_R)$  is a fixed point of maximum stress at the reference SIF  $K_R$ ,  $\xi = x/x_m$ , and  $\dot{x}_m = dx_m/dt$ . Eq. (8) shows that dynamic load with  $\dot{x}_m \propto K^\bullet > 0$  delays hydrogen accumulation in FPZ and this is opposite to the accelerating effect of positive stress gradient which arises after exceeding of some load level. In addition, negative stress gradient existing at lower loads due to precracking residual stress (cf. Fig. 1) also hinders hydrogenation.

#### DIFFUSION CALCULATIONS

Obviously  $x_c \leq x_m$ , and evaluation of  $C(x_m, t)$  yields conservative assessment of the role of load dynamics on FPZ hydrogenation. To illustrate the effect, the boundary-value problem (Eqs. (5), (8)) was solved numerically using the DuFort–Frankel scheme. Physical parameters were realistic for steels like AISI 4340 (cf. (2,9,11)):  $D = 10^{-13} \text{ m}^2/\text{s}$ ,  $V_H = 2 \text{ cm}^3/\text{mol}$ ,  $E = 190 \text{ GPa}$ ,  $\sigma_Y = 950 \text{ MPa}$ ,  $K_{max} = 35 \text{ MPa}\sqrt{\text{m}}$ , candidate threshold SIF value  $K_R = 40 \text{ MPa}\sqrt{\text{m}}$  and SSRT rate  $K^\bullet = 0.015 \text{ MPa}\sqrt{\text{m}}/\text{min}$ . For comparison, diffusion under sustained load was considered at the same SIF  $K_R$  (Fig. 2,3). For this case simulation confirms that the long-time approximation of Eq. (6) renders overestimation of hydrogenation rate. From numerical solution follows the stronger bounding for the time to attain 95% of the steady state  $\tau_{ss} = Dt_{ss}/x_R^2 \approx 230$  (Fig. 3). This is about the same as the time to attain  $K_R$  in SSRT,  $\tau_R = Dt_R/x_R^2 = 243$ . During SSRT concentration in moving point of maximum stress  $x = x_m(t)$  is lower than under sustained load (Fig. 2, 3). Whilst  $K(t) \leq K_{max}$ , concentration closely follows after hydrostatic stress evolution which is slow enough that diffusion practically maintains equilibrium hydrogen saturation  $C_\infty(K, x)$  at  $x \leq x_m(K)$  for instantaneous stress field  $\sigma(K(t), x)$ . Note, that up to  $K = K_{max}$  in the more distant reference point  $x_R > x_m$  concentration is even less. When  $K > K_{max}$  both evolution of stress field and shift of maximum stress position beyond the tip become more speedy due to acceleration of CTOD according to Eq. (2) in comparison to Eq. (7) valid before. At certain values of

stress redistribution parameters in SSRT, some uplift of concentration above the steady-state level may occur, although soon the delay of hydrogenation behind rapidly evolving stress state becomes notable as the main trend.

### CONCLUSION

The influence of transient stress fields on hydrogen diffusion near crack tip was theoretically modelled with relevance to the accelerated techniques of HAC testing.

Hydrogen accumulation in prospective fracture sites near crack tip during initial stage of SSRT up to maximum SIF of the crack prehistory displays low sensitivity to loading rate (in terms of SIF rate) and strong dependence on residual stress field produced at precracking, although this fact needs more precise evaluation. When near tip straining proceeds beyond the extends of the residual plasticity influence, the role of loading rate becomes more spectacular. It depends on diffusion coefficient of hydrogen and on the location of responsible material cells where microfracture proceeds, as well as on characteristics of material plasticity which define near tip stress field at each instantaneous load level.

*Acknowledgements.* This work was funded by the Spanish DGICYT (Grant UE94-001) and Xunta de Galicia (Grants XUGA 11801A93 and XUGA 11801B95). One of the authors (VKh) is also indebted to the Spanish Office of NATO (Scientific Affairs Division) and DGICYT (Grant SAB95-0122) for supporting his stay as a visiting scientist at the University of La Coruña (Spain).

### REFERENCES

- (1) Hirth, J.P. and Johnson, H.H., Corrosion, Vol. 32, 1976, pp.3-15.
- (2) Panasyuk, V. and Kharin, V., "Environment Assisted Fatigue (EGF 7)", MEP, London, 1990, pp. 123-144.
- (3) Toribio, J. and Kharin, V., "Materials Ageing and Component Life Extension", EMAS, Warley, Vol. 2, 1995, pp.931-940.
- (4) Van Leeuwen, H.-P., Eng. Fract. Mech., Vol. 6, 1974, pp.141-161.
- (5) Turnbull, A., Brit. Corros. J., Vol. 27, 1992, pp.271-289.
- (6) McMeeking, R.M. and Parks, D.M., "Elastic-Plastic Fracture (ASTM STP 668)", ASTM, 1979, pp. 175-194.
- (7) Gortemaker, P.C.M., de Pater, C. and Spiering, R.M.E.J., "Advances in Fracture Research (ICF5)", Pergamon Press, Oxford, Vol. 1, pp. 151-160.
- (8) Kanninen, M.F. and Popelar, C.H. "Advanced Fracture Mechanics", Oxford Univ. Press, New York, 1985.
- (9) Panasyuk, V., Andereikiv, A. and Kharin, V. Soviet Mater. Sci., Vol. 17(4), 1981, pp. 61-75.
- (10) Zhang, X., Chan, A.S.L. and Davies, G.A.O., "Computational Plasticity: Fund. and Appl.", Pineridge Press, Swansea, 1992, pp. 1561-1572.
- (11) Mayville, R.A., Warren, T.J. and Hilton P.D., J. Test. Eval., Vol. 17, 1989, pp. 203-211.

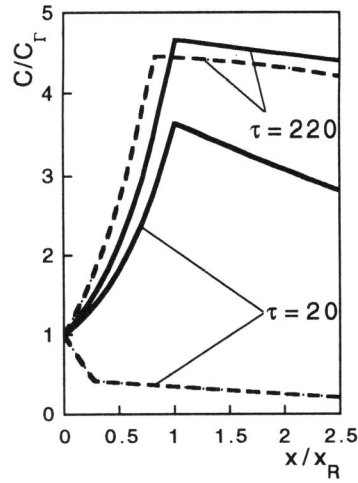
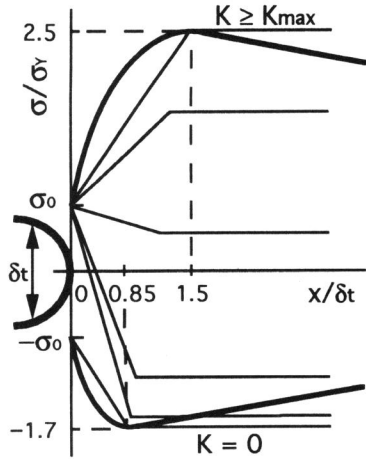


Figure 1 Evolution of hydrostatic stress in the vicinity of crack tip

Figure 2 Concentration at sustained load (solid lines) and SSRT (dashed)

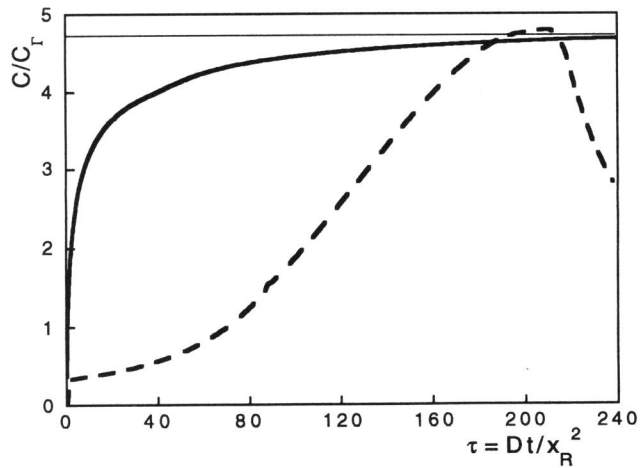


Figure 3 Concentration evolutions in maximum stress location  $x = x_m$  under sustained load (solid line) and SSRT (dashed line) to attain the steady-state level  $C_\infty$  (horizontal line)